An active interferometer-stabilization scheme with linear phase control

Vishnu Vardhan Krishnamachari[1], Esben Ravn Andresen[2], Søren Rud Keiding[3], and Eric Olaf Potma[1]

[1]*Department of Chemistry & Beckman Laser Institute, University of California at Irvine, Irvine, CA 92697, USA*

[2]*Department of Physics and Astronomy, University of Aarhus, Ny Munkegade, Building 1520, DK-8000 Aarhus C, Denmark*

[3]*Department of Chemistry, University of Aarhus, Langelandsgade 140, DK-8000 Aarhus C, Denmark*

epotma@uci.edu

Abstract: We report a simple and robust computer-based active interferometer stabilization scheme which does not require modulation of the interfering beams and relies on an error signal which is linearly related to the optical path difference. In this setup, a non-collinearly propagating reference laser beam stabilizes the interference output of the laser light propagating collinearly through the interferometer. This stabilization scheme enables adjustable phase control with 20 ms switching times in the range from 0.02π radians to 6π radians at 632.8 nm.

OCIS codes: 120.3180 (Interferometry); 120.5050 (Phase measurement); 260.3160 (Interference)

References and links

1. M. B. Gray, D. E. McClelland, M. Barton, and S. Kawamura, "A simple high-sensitivity interferometric position sensor for test mass control on an advanced LIGO interferometer," Opt. Quant. Electron. **31**, 571-582 (1999).
2. K. A. Jensen, R. J. Larson, S. D. Bergeson, and E. F. McCormack "Exploring closed-loop feedback control using experimenets in optics," arXiv:physics (2001) http://www.citebase.org/cgi-bin/citations?id=oai:arXiv.org:physics/0106091 .
3. A. A. Freschi, and J. Frejlich, "Adjustable phase control in stabilized interferometry," Opt. Lett. **20**, 635-637 (1995).
4. M. C. Barbosa, I. de Oliveira, and J. Frejlich, "Feedback operation for fringe-locked photorefractive running hologram," Opt. Commun. **201**, 293-299 (2002).
5. H. Iwai, C. FangYen, G. Popescu, A. Wax, K. Badizadegan, R. R. Dasari and M. S. Feld, "Quantitative phase imaging using stabilized phase-shifting low-coherence interferometery," Opt. Lett. **29**, 2399-2401 (2004).
6. P. Horowitz, and W. Hill, *Art of Electronics* (Cambridge University Press, New York, 2nd Ed., 1989)
7. J. Bechhoefer, "Feedback for physicists: A tutorial essay on control," Rev. Mod. Phys. **77**, 783-836 (2005).
8. E. O. Potma, C. L. Evans, and X. S. Xie, "Heterodyne coherent anti-Stokes Raman scattring (CARS) imaging," Opt. Lett. **31**, 241-243 (2006).

1. Introduction

In interferometric and holographic applications, it is often necessary to maintain a constant phase difference between the beams in the two arms of an interferometer. In applications such as phase-shifting interferometry, the capability to adjust the phase difference to an arbitrary value is also required. In either of these cases, various stabilization techniques are used which

rely on generating an error signal based on the intensity output of the interferometer. This error signal is in turn processed and fed back to a phase-adjusting element in the interferometer.

Gray et al. [1] developed an active stabilization scheme which employs two detectors to detect the intensity at the output ports of a Michelson interferometer. The difference between these two signals, being proportional to the cosine of the phase difference, was used as an error signal to lock the interferometer at a position close to the center of a particular fringe. A similar technique has also been reported by Jensen et al. [2]. However, these DC-coupled balanced stabilization techniques do not permit locking of the interferometer at arbitrary phase values. The most commonly used stabilization technique with adjustable phase control is based on applying a phase modulation at a frequency Ω to one of the interfering beams and subsequently detecting the output signals using lock-in techniques at frequencies Ω and 2Ω. Using this scheme, in which the error voltage is proportional to the sine of the phase difference between the beams, Freschi and Frejlich were able to stabilize an interferometer at different phase settings with a precision better than one degree [3]. This stabilization scheme has found many applications in holography [4] and phase-shifting low-coherence interferometry [5].

However, in either of the above described techniques, the error signal is nonlinear, being proportional to the (co)sine of the phase difference between the interfering beams rather than the phase difference itself. Hence, if the phase difference between the beams jumps beyond $\pm\pi$ radians (due to, say, external perturbations), the interferometer gets locked to a neighboring fixed point displaced by 2π radians. This is undesirable in applications where multiple wavelengths are being guided through the interferometer and where the absolute phase difference needs to be maintained at a fixed value. Also, the second harmonic locking technique [3] is less attractive in applications with signal acquisition rates faster than the modulation frequency.

In this article, we report a technique that generates an interferometric error signal linearly related to the phase difference ($\Delta\phi$) between the two arms of a Mach-Zehnder interferometer, and present a computer-based stabilization scheme for adjustable phase control. In this technique, a stabilizing reference laser source is propagated in non-collinear geometry and two photodiodes are used to detect the interference signals that are in quadrature. This enables calculation of the tangent of the phase difference and hence $\Delta\phi$ itself by performing the arctangent operation using a computer. The highlights of this technique include (a) no additional modulation of the interfering beams (b) the stabilization can be achieved at arbitrary optical phase differences with no limitations of $\pm\pi$ phase jumps and (c) a wedge plate is used to configure the interferometer such that a narrow-band beam is collinearly guided through the interferometer while the reference beam used to stabilize it propagates in a non-collinear fashion. We demonstrate the performance of this scheme by measuring the stability of the interference signal generated by a picosecond laser beam propagating collinearly through the interferometer.

2. Interferometer – Collinear and non-collinear geometry

Figure 1 shows a sketch of the experimental setup. A He-Ne laser operating at 632.8 nm is used as a reference (r) source to stabilize the interferometer. A 822 nm laser beam (p-beam) from a tunable intra-cavity doubled optical parametric oscillator (OPO, Levante, APE Berlin: pulse width = 5 ps, and repetition rate = 76 MHz) is chosen as the primary light source; the aim is to stabilize the interference signal from this light source. The beam splitter BS1 splits the collimated beams (r into r_1, r_2, and p into p_1, p_2) into the two arms of the interferometer. In the first arm, both the beamlets (r_1 and p_1) co-propagate and are individually detected at the two output ports after the beam splitter BS2 using a pair of interference filters (F). A mirror mounted on a piezo stack is used to actively stabilize the interferometer.

The second arm of the interferometer is similar to that of the first except for a wedge plate (W) placed in the beam path to disperse r_2 and p_2. The orientation of W is adjusted so as to allow

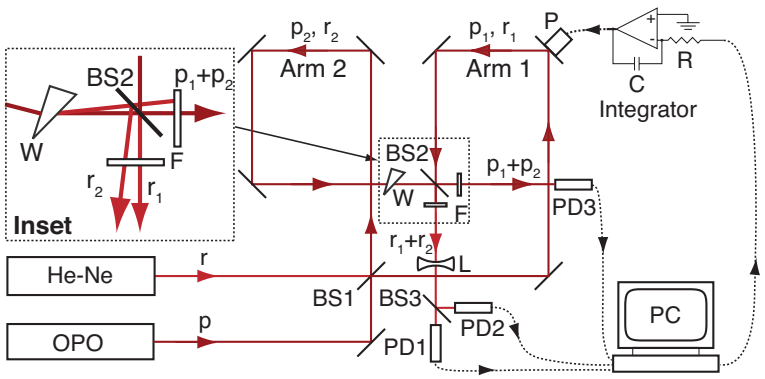

Fig. 1. Schematic of the experimental setup employing He-Ne laser as reference (r) laser to stabilize the interferometer. BS1, BS2, BS3: beamsplitters; F: interference filters; W: wedge plate; PD1, PD2, PD3: photodiodes; L: diverging lens; P: piezo (AE0505D08, Thorlabs Inc.) ; R = 20 kΩ; and C = 6 F. The angles of the beams (exaggerated) reflected and transmitted at BS2 after passing through the wedge plate are depicted in the inset.

collinear propagation of p_1 and p_2 after BS2 (see the inset in Fig. 1); the resulting interference intensity is detected using a photo-diode PD3. At the second output port of the interferometer, the r_2-beamlet reflected at BS2 exits at an angle with respect to r_1 (see the inset in Fig. 1; the angles shown in the figure are exaggerated). Due to this non-collinear geometry of propagation of the reference beamlets, straight line fringes are observed beyond the diverging lens (L). Two distinct points on the fringe pattern that are displaced from each other by one-fourth of the fringe spacing are detected by the photodiodes PD1 and PD2 placed at equal distances from the beamsplitter BS3. Note that the reference laser in this scheme has to be of different wavelength than that of the primary light source.

The voltage values generated by the photodiodes PD1, PD2 and PD3 are sampled at 5 kHz using a National Instruments data acquisition board (Model: PCI-6221) and the signals are stored in a computer (PC) for further processing. The detection bandwidth of this stabilization scheme is ultimately limited by the sampling time (≈ 0.2 ms) of the computer and the speed of stabilization (without overshoot) is limited by the piezo response time (≈ 20 ms).

3. Stabilization scheme

The stabilization of the interferometer is performed in two steps: (*i*) calibration and (*ii*) phase determination for feedback control.

3.1. Calibration

The first sub-step in the calibration process involves proper positioning of the photodiodes. This is achieved by applying a voltage ramp to the piezo (which induces $0-4\pi$ radians of phase change in the first arm of the interferometer) and simultaneously translating one of the photodiodes laterally till the interference signals detected by them are in quadrature. In the second sub-step, with the voltage ramp to the piezo still on, the time varying sinusoidal signals detected at PD1 and PD2 are analyzed to determine their amplitudes of oscillation ($\mathscr{A}_1$ and $\mathscr{A}_2$) and their offset levels ($\mathscr{O}_1$ and $\mathscr{O}_2$). Subsequently, the incoming signals are normalized to oscillate between ± 1. In our experiment, this calibration process is performed using a home-written C++ software based on an iterative procedure. Provided the photodiodes are in the right positions, this process of calibration is done in under two seconds.

3.2. *Phase determination & control via feedback*

With the calibration process complete, the free-running output due to the interference between r_1 and r_2 detected at PD1 and PD2 can be written as

$$V_1 = \mathscr{O}_1 + \mathscr{A}_1 \sin\Delta\phi \quad (1)$$

$$V_2 = \mathscr{O}_2 + \mathscr{A}_2 \cos\Delta\phi \quad (2)$$

where $V_{1,2}$ are the detected voltages, $\Delta\phi$ is the phase difference between the two arms of the interferometer induced by acoustic noise and environmental perturbations and $\mathscr{O}_{1,2}$ and $\mathscr{A}_{1,2}$ are the offset and the amplitude values calculated in the previous step. Hence, the phase difference can be obtained using the formula:

$$\Delta\phi = \mathscr{U}\left\{\arctan\left(\frac{V_1-\mathscr{O}_1}{V_2-\mathscr{O}_2}\times\frac{\mathscr{A}_2}{\mathscr{A}_1}\right)\right\} \quad (3)$$

where $\mathscr{U}$ is the phase unwrapping operation which ensures that $\Delta\phi$ is proportional to optical path change. The unwrapping operation works efficiently as long as the optical path change does not change more than half wavelength (π radians @ 632.8 nm) within a sampling period. In practice, this condition is always fulfilled since all the optical path variations in our setup are slower than the sampling frequency. If $\Delta\phi_d$ is the desired phase difference at which the interferometer is required to be locked, then the error signal, e, is

$$e = g\times(\Delta\phi - \Delta\phi_d) \quad (4)$$

where g is a constant gain factor. The error signal given in Eq. (4) forms the input to a simple operational-amplifier-based integral feedback circuit [6] which in turn generates a compensation signal for driving the piezo (see [7] for a general account of feedback control).

4. Experimental results

Using a C++-based GUI software, we can change the gain factor g, set the desired phase difference $\Delta\phi_d$ to an arbitrary value, and perform adjustable phase control. In the following subsections we demonstrate the speed and robustness of this stabilization scheme.

4.1. *Stabilization with linear error signal*

As mentioned in the previous sections, the strength of the current stabilization scheme is the generation of a linear error signal. To verify the linearity of the error signal, the optical path difference was changed by applying a triangular waveform to the piezo with $\Delta\phi_d$ set to zero. The generated error signal is plotted in Fig. 2. As is evident from the figure the linear relationship between the two quantities is valid for more than 2 m (which is $> 6\pi$ radians @ 632.8 nm) path length variation.

Fig. 3(a) shows the free-running output of the interferometer. The output intensities drift due to variations in the optical path difference between the two arms. Figure 3(b) shows the long term stability of the interferometer with the feedback switched on and with $\Delta\phi_d$ set to zero radians. The freely drifting photodiode outputs settle within 20 ms. Note that the PD1 and PD2 outputs are $\frac{\pi}{2}$ out-of-phase as required.

Figure 4 shows the normalized spectra of the OPO interference signal in the absence and in the presence of the stabilization. In the free-running mode of the OPO, the output intensity, apart from a slow drift, is influenced by the acoustic noise of the chillers and the pumps in our laboratory. However, these acoustic disturbances are suppressed when the stabilization mechanism is switched on as is evident from Fig. 4. The estimated mean standard deviation of the

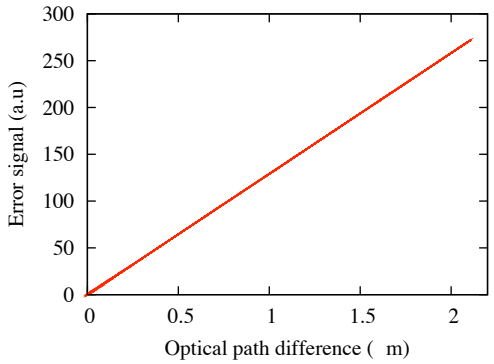

Fig. 2. Recorded linear dependence of the error signal on the optical path difference between the two beams (refer to Eqs. (3) and (4)).

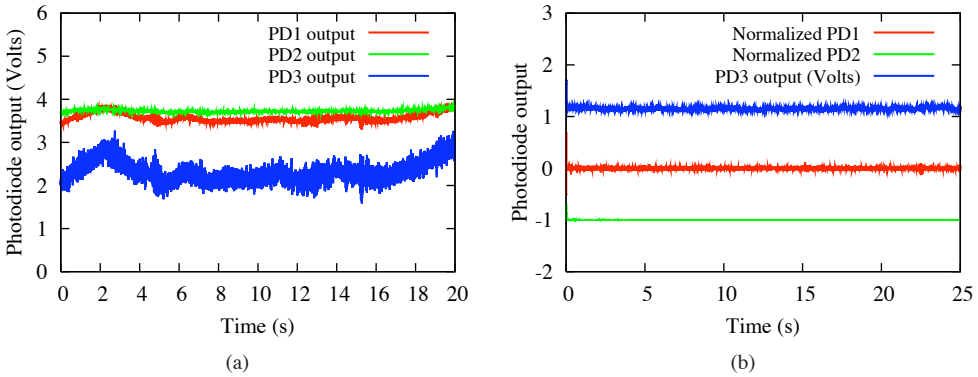

Fig. 3. (a) Free-running output from the interferometer. (b) Stabilized output of the interferometer locked at $\Delta\phi_d = 0$.

noise in the stabilized OPO signal corresponds to an optical path variation of ≈ 6.5 nm. We note that this limitation is not imposed by the stabilization scheme but rather by the structured acoustic noise spectrum in our laboratory. The performance can be improved by implementing a more sophisticated feedback control loop.

Another important aspect of any stabilization scheme is the speed with which the states of stabilization can be switched. We determined the optimum response time, devoid of signal overshoot, to be 20 ms for a gain $g = 20$ and for phase changes below π radians.

4.2. Adjustable phase control

Figure 5(a) demonstrates the real-time phase adjustable feature of the stabilization scheme. Every 2 s the desired phase difference value was increased by 0.2π radians (@ 632.8 nm) with a total phase variation of 5π radians in 50 s. Due to the linear dependence of the error signal, the interferometer can be promptly locked at arbitrary phase values even for phase settings beyond π radians. Figure 5(b) shows the interference output of OPO when the desired phase, $\Delta\phi_d$ is instantly switched at $t = 4$ s from zero radians to $\pi, 2\pi, 3\pi$, and 4π radians (@ 632.8 nm). For comparison, the normalized output at PD1 is also shown. The interferometer gets readily locked for phase changes as large as 4π radians. This is possible because (a) the stabilization mechanism is based on an error signal which is directly proportional to the optical path differ-

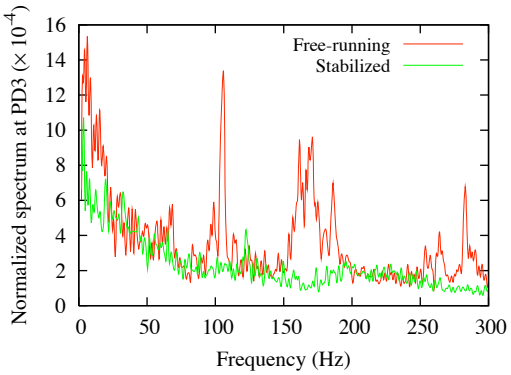

Fig. 4. Normalized Fourier spectra of the OPO interference output in the absence (red line) and the in the presence (green line) of stabilization.

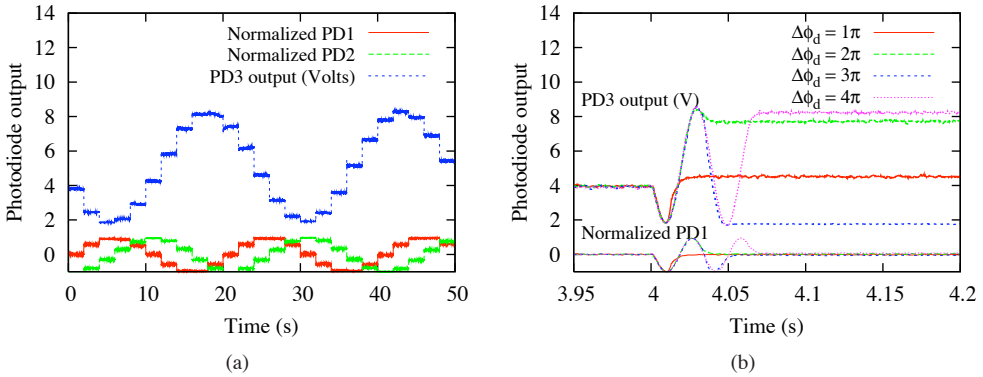

Fig. 5. Demonstration of adjustable phase control: (a) $\Delta\phi_d$ was changed in steps of 0.2π @ 632.8 nm every 2 s; the net phase change in 50 s is about 5π radians; the gain factor was chosen to be 20. (b) Switching the optical phase difference from 0 radians to π, 2π, 3π, and 4π radians respectively.

ence and (b) the phase unwrapping procedure works efficiently since the computer sampling time (≈ 0.2 ms) is much smaller than the response time of the piezo (≈ 20 ms).

The above results clearly establish the robustness of the stabilization scheme. The idea of linear error signal generation and the technique for driving the interferometer in collinear and non-collinear geometries simultaneously are general and hence can be used for the stabilization of any interferometric configuration without additional modulation of the interfering beams. We employ this scheme to stabilize a multi-wavelength interferometer for performing phase-sensitive imaging using heterodyne coherent anti-Stokes Raman scattering (CARS) imaging [8] with picosecond pulses.

5. Conclusion

We have demonstrated a simple and robust interferometric stabilization scheme in which the error signal generated for stabilization is linear with respect to the changes in the optical path length of the interferometer. It allows for locking the interferometer at arbitrary path differences ranging from a few nanometers to at least 2 m with switching times down to 20 ms.